Published OnlineFirst November 5, 2010; DOI: 10.1158/0008-5472.CAN-10-2591

Tumor and Stem Cell Biology

Cancer Research

CXCR4 Signaling Regulates Metastasis of Chemoresistant Melanoma Cells by a Lymphatic Metastatic Niche

Minah Kim[1,2], Young Jun Koh[1,3], Kyung Eun Kim[1,4], Bong Ihn Koh[1,2], Do-Hyun Nam[5], Kari Alitalo[6], Injune Kim[1,3], and Gou Young Koh[1,2,3,4,5]

Abstract

Highly metastatic and chemotherapy-resistant properties of malignant melanomas stand as challenging barriers to successful treatment; yet, the mechanisms responsible for their aggressive characteristics are not fully defined. We show that a distinct population expressing CD133 (Prominin-1), which is highly enriched after administration of a chemotherapeutic drug, dacarbazine, has enhanced metastatic potential *in vivo*. $CD133^+$ tumor cells are located close to tumor-associated lymphatic vessels in metastatic organs such as the regional lymph nodes and lung. Lymphatic endothelial cells promote the migratory activity of a $CD133^+$ subset to target organs and regulation of lymphatic growth efficiently modulates the metastasis of $CD133^+$ tumor cells. We found that lymphatic vessels in metastatic tissues stimulate chemokine receptor 4 $(CXCR4)^+/CD133^+$ cell metastasis to target organs by secretion of stromal cell–derived factor-1 (SDF-1). The $CXCR4^+/CD133^+$ cells exhibited higher metastatic activity compared with $CXCR4^-/CD133^+$ cells and, importantly, blockade of CXCR4 coupled with dacarbazine efficiently inhibited both tumor growth and metastasis; dacarbazine alone could not attenuate tumor metastasis. The current study demonstrates a previously unidentified role of the lymphatic microenvironment in facilitating metastasis of chemoresistant melanoma cells via a specific chemotactic axis, SDF-1/CXCR4. Our findings suggest that targeting the SDF-1/CXCR4 axis in addition to dacarbazine treatment could therapeutically block chemoresistant $CD133^+$ cell metastasis toward a lymphatic metastatic niche. *Cancer Res; 70(24); 10411–21. ©2010 AACR.*

Introduction

Malignant melanoma is highly metastatic and notoriously resistant to conventional therapies, posing a challenging therapeutic obstacle attributed to tumor population heterogeneity (1, 2). Numerous clinical approaches have been suggested, including chemotherapy and immunologic therapies, for treating melanoma (3, 4), but they have yet to produce a remarkable therapeutic effect. Response rates to dacarbazine, the most widely used agent for melanoma treatment, are significantly low at 10% to 25% (5) and its administration can rather enhance metastatic potential as well as tumorigenic properties *in vivo* (6). Although several molecular mechanisms for drug resistance have been evaluated, such as increased DNA repair and cytokine expression in melanoma, resistance to chemotherapy, and an induced, aggressive metastatic phenotype remain as major challenges for melanoma treatment.

The existence of a rare tumor-initiating subpopulation that exhibits resistance to conventional cancer therapies has been proposed (7, 8). Recent studies in melanoma have addressed a possible mechanism for tumor chemoresistance, identifying drug transporter ABCB5 as a critical mediator of tumor initiation as well as chemoresistance (9, 10). Although the rarity of tumorigenic cells identified by specific surface markers has been challenged, especially in the context of melanoma (11–13), it remains unanswered whether distinct subpopulations are more responsible for chemoresistance than a heterogeneous population. Also, the molecular features that characterize chemoresistant cells require further investigation.

Metastasis occurs in an organ-specific and highly organized manner. Certain tumors are prone to metastasize to preferred sites by diverse determinants such as intrinsic properties of tumor cells and circulation patterns (14). Increasing evidences have shown that the microenvironment at metastatic sites can modulate metastatic potential (15). The molecular basis of organ-specific metastasis is poorly understood, but local

Authors' Affiliations: [1]National Research Laboratory of Vascular Biology and Stem Cells, Departments of [2]Biological Sciences, [3]Graduate School of Medical Science and Engineering; [4]Graduate School of Nanoscience and Technology (WCU), Korea Advanced Institute of Science and Technology (KAIST), Daejeon, and [5]Institute for Refractory Cancer Research Program, Samsung Medical Center, Sungkyunkwan University School of Medicine, Seoul, Korea; and [6]Molecular/Cancer Biology Laboratory and Haartman Institute, University of Helsinki, FI-00014, Helsinki, Finland

Note: Supplementary data for this article are available at Cancer Research Online (http://cancerres.aacrjournals.org/).

Corresponding Author: Gou Young Koh, Department of Graduate School of Medical Science and Engineering, KAIST, 373-1, Guseong-dong, Daejeon, 305-701, Korea. Phone: 82-42-350-2638, Fax: 82-42-350-2610. E-mail: gykoh@kaist.ac.kr

doi: 10.1158/0008-5472.CAN-10-2591

Published OnlineFirst November 5, 2010; DOI: 10.1158/0008-5472.CAN-10-2591

microenvironmental components of metastatic sites can create a conducive niche for attracting tumor cells to favorable organs (16). Chemokine-mediated mechanisms also govern the pattern of metastasis to specific target organs, in that the local expression of chemoattractants may guide chemokine receptor–expressing tumor cells to specific target organs (17–19). In addition to using blood vessels, solid tumors can also utilize the lymphatic vasculature to disseminate tumor cells to distant sites (20–22). In malignant melanoma, lymphatic vessels represent the major route of metastatic dissemination (23). Lymph node (LN) metastasis is the first step of tumor dissemination for a variety of human cancers including melanoma. Although the degree of LN metastasis has long been one of the criteria for determining the prognosis of human cancers, the molecular mechanisms of lymphatic metastasis are poorly understood (24). Whether the LNs encourage tumor cell dissemination for further systemic metastasis also remains to be determined. However, the LNs may provide a supportive environment for tumor metastasis by increasing the metastatic propensity of tumor cells (15). Regulation of lymphatic vessel growth also affects pulmonary metastasis, beyond regional LN metastasis, in mouse models of some cancers (25, 26). Vascular growth factor (VEGF)-C, a lymphangiogenic factor, directly induces lung lymphangiogenesis which promotes intralymphatic spread in the lungs (27).

Our goal was not to wade into the controversy about the presence of melanoma stem cells to seed cancer growth but rather to determine underlying mechanisms mediating active metastasis of chemoresistant melanoma cells to specific target organs. Here, we demonstrate that a lymphatic microenvironment at metastatic sites promotes the recruitment of disseminating tumor cells with a particular affinity for CD133-positive tumor cells, which are highly enriched after cytotoxic drug treatment *in vivo*. Furthermore, we identify the stromal cell–derived factor 1 (SDF-1)/chemokine receptor 4 (CXCR4) axis to play a critical role in mediating metastasis of a chemoresistant tumor subpopulation toward a lymphatic niche in specific target organs, regional LNs and lungs.

Materials and Methods

Mice and tumor model

C57BL/6J mice were purchased from Jackson Laboratory and bred in our pathogen-free animal facility. K14-VEGF-C transgenic mice (FVB/N genetic background) were generated, maintained as previously described (28), and transferred to KAIST. They were backcrossed with the C57BL/6J strain for F10–F11 generations before being used for this study. Animal care and experimental procedures were performed under the approval of the Animal Care Committee of KAIST. Mouse cell line B16/F10 melanoma was obtained from American Type Culture Collection (ATCC). The cell line was cultured in Dulbecco's modified Eagle's medium (DMEM; Gibco BRL) containing 10% heat-inactivated fetal bovine serum (FBS; HyClone), penicillin, and streptomycin (Sigma-Aldrich) in plastic tissue culture dishes (Nunc) at 37°C in a humidified atmosphere of 5% CO_2. To generate a melanoma model, 1×10^6 of B16/F10 cells (resuspended in 100 μL of PBS) or indicated number of sorted subpopulations from tumor were orthotopically injected into intradermal dorsal skin of 7- to 8-week-old male mice.

Tissue collection and histologic analysis

On the indicated days after tumor implantation or the treatments, mice were anesthetized by intramuscular injection of a combination of anesthetics (80 mg/kg of ketamine and 12 mg/kg of xylazine), and the size of tumors was measured. Mice were perfused with PBS before tumors and other tissues, including LNs, lungs, livers, and diaphragms, were harvested. Tissues were fixed with 100% acetone at −20°C for 12 hours, paraffin-embedded and sectioned (thickness = 10 μm). After blocking with 5% goat serum in PBST (0.3% Triton X-100 in phosphate-buffered saline) for 1 hour at room temperature, the samples were incubated overnight at 4°C with 1 or more of the following primary antibodies: rat anti-mouse lymphatic vessel endothelial hyaluronan receptor-1 (LYVE-1; Aprogen), rabbit anti-mouse LYVE-1 (AngioBio), hamster anti-mouse CD31 (Millipore), rat anti-mouse PNAd (BD Biosciences Pharmingen), rabbit anti-mouse CD133 (Abcam), rat anti-mouse CD133 (eBioscience), mouse anti-MelanA (Abcam), mouse anti-nestin (Abcam), rat anti-mouse CD166 (eBioscience), rat anti-mouse CXCR4 (BD Biosciences Pharmingen), rat anti-mouse CXCR4 (R&D systems), rabbit anti-mouse CXCL12 (eBioscience), rabbit anti-human Prox-1 (ReliaTech), hamster anti-mouse podoplanin (AngioBio), or anti-mouse SMA-α (Sigma). After several washes in PBST, the samples were incubated for 2 hours at room temperature with the fluorescence-conjugated secondary antibodies.

Fluorescent signals were visualized and digital images were obtained using a Zeiss inverted microscope, ApoTome microscope, or LSM 510 confocal microscope equipped with argon and helium–neon lasers (Carl Zeiss). The morphometric measurements of blood vessels and lymphatic vessels in tumors and LNs and metastatic cells in LNs and lungs were made on sectioned tissues with immunostaining using photographic analysis in ImageJ software (http://rsb.info.nih.gov/ij) or a Zeiss ApoTome microscope coupled to a monochrome charge-coupled device (CCD) camera and image analysis software (AxioVision, Zeiss). The number of metastasized $CD133^+$/$MelanA^+$ tumor cells in the axillary LN (ALN) was measured on the mid-section. The measurements of $MelanA^+$ metastatic tumor colonies (>20 $MelanA^+$ cells) in the lungs of the tumor-bearing mice were made on the 3 randomly chosen sections. Density measurements of LYVE-1^+ lymphatic vessels and $CD31^+$ blood vessels in the tumors were made on 3 fields in the intratumoral and peritumoral regions at a screen magnification of 100×, each 5.25 mm^2 in area.

Flow cytometric analysis and sorting

Tumor tissues and lymph nodes were washed in PBS and digested using 0.2% collagenase type-IV (Worthington) for 1 hour at 37°C. After digestion, cells were filtered 2 times by 40-μm nylon meshes to remove cell clumps. Peripheral blood was collected in a tube containing EDTA by cardiac puncture under anesthesia. Red blood cells (RBC) were removed from

Published OnlineFirst November 5, 2010; DOI: 10.1158/0008-5472.CAN-10-2591

the peripheral blood using a RBC lysis buffer (Sigma) before flow cytometric analysis. Cells were resuspended in Hank's-buffered salt solution (HBSS) containing 2% FBS and stained for 20 minutes on ice with 1 or more of the following antibodies: anti-mouse CD133 antibody (13A4, eBioscience), anti-mouse CXCR4 antibody (BD Biosciences Pharmingen), anti-mouse CD45 antibody (30-F11, eBioscience), anti-mouse CD31 antibody (BioLegend), anti-mouse VEGFR-2 antibody (eBioscience), or anti-mouse VEGFR-3 antibody (eBioscience). Dead cells were excluded by 7-aminoactinomycin D (7-AAD; (Invitrogen). For sorting, cells were stained with above antibodies and sorted using fluorescence activated cell sorting (FACS) Aria II (Becton Dickinson). Data were analyzed by using FlowJo software (Tree Star).

Migration assay and coculture study

For migration assays, 1×10^5 of HEK-293E cells (ATCC), primary cultured HUVECs and lymphatic endothelial cells (LEC; within 7–8 passages; Cambrex) were resuspended in 27 μL of DMEM containing 2% FBS and seeded in the lower well of a Boyden Chamber before a polycarbonate membrane was placed (8-μm pore size; Neuro Probe). A total of 2×10^4 of sorted $CD133^+$ or $CD133^-$ cells, which were resuspended in 50 μL of the same medium, were seeded in the upper chamber. After 24 hours of incubation at 37°C, the nonmigrated cells on the top of the filter were removed and the migrated cells on the bottom of the filter were stained in hematoxylin and eosin solution. The number of stained cells was counted under a microscope. For a Matrigel coculture study, 2.5×10^4 of LECs were resuspended in DMEM containing 2% FBS. A total of 1×10^4 of sorted $CD133^+$ or $CD133^-$ cells from tumor were prelabeled with 5-(and-6)-carboxyfluorescein diacetate, succinimidyl ester (CFDA SE; Invitrogen) and cocultured with LECs on a Matrigel (60 μL per well)-coated 8-well chambered slide (Nunc). For CXCR4 blocking experiments, 500 ng/mL of the CXCR4 blocking antibody (R&D Systems) was treated after seeding of mixed cells. After 24 hours of incubation at 37°C, LECs and either prelabeled $CD133^+$ or $CD133^-$ cells were visualized using a Zeiss LSM 510 confocal microscope.

Quantitative real-time PCR

Total RNA was extracted from the indicated cells and tissues using an Easy-BLUE Total RNA Extraction Kit (iNtRON Biotechnology) according to manufacturer's instructions. Each cDNA was made with SuperScript II Reverse Transcriptase (Invitrogen), and quantitative real-time PCR was performed with the indicated primers (Supplementary Table 1) using iCycler (Bio-Rad) equipped with iQ5 (Bio-Rad). The real-time PCR data were analyzed with Bio-Rad iQ5 Optical System Software (Bio-Rad).

Drug treatment

Seven days after tumor implantation, drug treatment was started. For dacarbazine treatment, a treatment cycle consisted of an intraperitoneal injection of dacarbazine (25 mg/kg, Sigma-Aldrich) after an epifocal application of dinitrochlorobenzene (dissolved in mixture of acetone and olive oil, 4:1) on the tumor. For the first cycle, the tumors were treated with 2% dinitrochlorobenzene; whereas, for the following cycles, 1% dinitrochlorobenzene was used. Cycles were repeated every 4 days. As a control, equal volumes of vehicle were administered in the same manner. To block CXCR4, 1.25 mg/kg of AMD3100 (Sigma-Aldrich) was subcutaneously administered every other day for 2 weeks. To block VEGF-C/D, 1×10^9 pfu of adenoviral delivery of soluble VEGFR-3 (Ad-sVEGFR-3) or Ad-βgal was intravenously delivered starting from 3 days after tumor implantation once a week for 3 weeks.

Statistical analysis

Values are presented as mean ± standard deviation (SD). Significant differences between means were determined by unpaired Student's *t* test or with 1-way ANOVA followed by the Student–Newman–Keuls test. Statistical significance was set at $P < 0.05$.

Results

A chemoresistant subpopulation expressing CD133 associates with lymphatic vessels in metastatic organs

Our preliminary study to see the effects of standard chemotherapy on melanoma metastasis following exposure of a chemotherapeutic agent, dacarbazine, showed that metastases in ALN as a regional LN and lung as distant metastatic organ were not attenuated even though tumor growth was reduced by 43% (Supplementary Fig. S1A–C).

Immunostaining of primary tumors and ALNs for the lymphatic marker, LYVE-1, showed a preferential increase of lymphatic vasculatures over blood vessels in dacarbazine-treated mice compared with vehicle-treated control (Supplementary Fig. S1D and F). However, any notable difference in the pericyte coverage of blood vessels was not detectable between dacarbazine-treated mice and vehicle-treated control (Supplementary Fig. S1E). Given these results, we sought to address the possibility of the chemotherapeutic treatment for melanoma leading to the enrichment of chemoresistant subpopulations that could actively metastasize in a lymphatic system-dependent manner. As a subpopulation expressing Prominin-1 (CD133) is enriched after therapeutic treatment in some cancers (7, 29), we examined the enrichment of $CD133^+$ tumor cells following exposure to dacarbazine after melanoma implantation. Remarkably, dacarbazine treatment *in vivo* elevated the frequency of the $CD133^+$ subpopulation by approximately 9-fold within the tumor population depleted of hematopoietic and endothelial progenitors relative to vehicle-treated mice, showing high resistance of the CD133-expressing subset to the chemotherapeutic drug (Fig. 1A and B).

We next examined the metastatic potential of the $CD133^+$ subpopulation to ALNs and distant organs such as the lungs. Flow cytometric analysis of homogenized lymph nodes after tumor implantation showed that $CD45^-/CD133^+$ cells consist of up to ~2.4% of total LN cells after $CD31^+$ endothelial cell depletion, whereas no $CD45^-/CD133^+$ cells were detectable in ALNs of control mice without tumor implantation (Supplementary Fig. S2A), implying that $CD133^+$ cells are highly metastatic in nature. In addition, the frequency of melanoma-derived

Published OnlineFirst November 5, 2010; DOI: 10.1158/0008-5472.CAN-10-2591

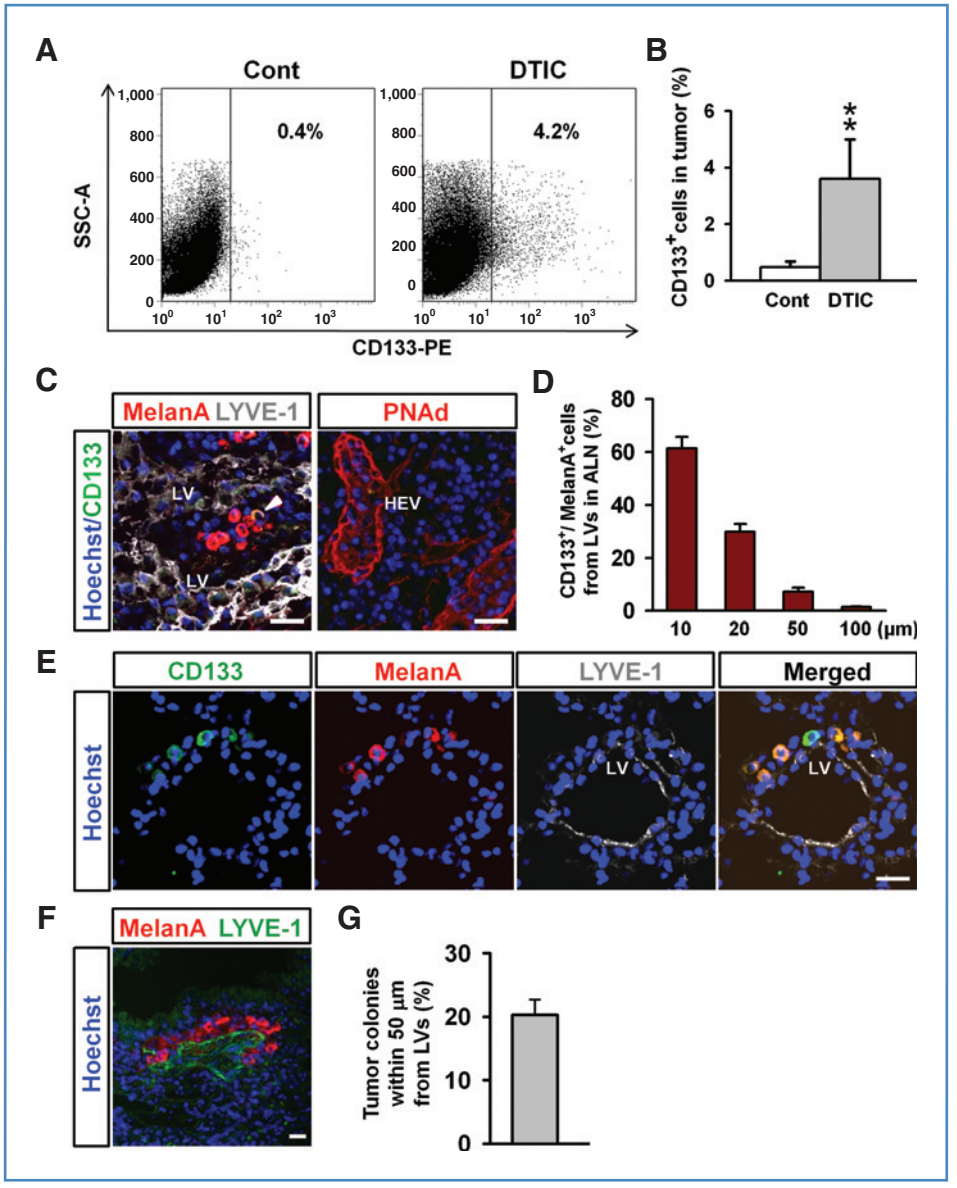

Figure 1. A chemoresistant subpopulation expressing CD133 associates with lymphatic vessels in metastatic organs. A and B, 7 days after B16/F10 melanoma cells were implanted into C57BL/6J mice, dacarbazine (DTIC, 50 mg/kg intraperitoneally) or vehicle treatment (Cont) was administered. Tumors were sampled 14 days after treatment. A, FACS analysis of $CD133^+$ melanoma cells in tumors after treatment of DTIC or Cont. B, quantification of the $CD133^+$ fraction in tumors. Each group, $n = 11$. **, $P < 0.01$ versus Cont. C–G, 3 weeks after B16/F10 melanoma cells were implanted into C57BL/6J mice, ALNs and lungs were sampled. C and D, images showing $CD133^+$/$MelanA^+$ tumor cells, LYVE-1^+ lymphatic vessels, and $PNAd^+$ HEVs in ALN (C) and percentage of $CD133^+$/$MelanA^+$ cells, which are located at indicated distances from the nearest LYVE-1^+ lymphatic vessels (LV), per total $CD133^+$/$MelanA^+$ cells in the mid-section of ALN (D). Arrowheads indicate $CD133^+$ melanoma cells. E, images showing $CD133^+$/$MelanA^+$ tumor cells and LYVE-1^+ lymphatic vessels in the lungs. F and G, image showing $MelanA^+$ cells around LYVE-1^+ lymphatic vessels on lung section (F) and percentage of tumor colonies (defined as >20 $MelanA^+$ cells that are localized as a cluster) within 50 μm from lymphatic vessels per total tumor colonies in the lung section (G). All nuclei are stained with Hoechst. Scale bars, 20 μm.

$CD45^-$/$CD133^+$ cells represented ~0.06% of the total peripheral blood cells, whereas $CD45^-$/$CD133^+$ cells were very rare, if at all detectable (<0.001%) in the peripheral blood of control mice (Supplementary Fig. S2B). Using an antibody for MelanA, which is prevalently expressed in melanocytes, we further found that 5.5% of metastasized $MelanA^+$ cells in ALNs at 3 weeks after melanoma cell implantation coexpressed CD133, whereas $MelanA^+$ cells were rarely detected in the ALNs of vehicle-injected control mice, confirming that the subpopulation expressing CD133 has high metastatic potential. Of note, $CD133^+$ tumor cells were closely associated with LYVE-1^+ lymphatic vessels compared with PNAd-positive high endothelial venules (HEVs; Fig. 1C and D). For the distant metastatic organ of melanoma, the lungs in particular, immunostaining showed that the metastasized $CD133^+$/$MelanA^+$ cells colocalize with other $MelanA^+$ tumor cells by forming colonies (a colony defined as >20 $MelanA^+$ cells). Interestingly, we observed a certain set of $CD133^+$ tumor cells closely encompass LYVE-1^+ lymphatic vessels (Fig. 1E and Supplementary Fig. S3B). We confirmed that LYVE-1^+ vessel structures are lymphatic vessels by coimmunostaining with Prox-1 or podoplanin (Supplementary Fig. S3A and B). Quantificational analysis showed that 20.2% of total $MelanA^+$ tumor colonies were located within 50 μm from lymphatic vessels (Fig. 1F and G). These results based on LN and lung metastases suggest that lymphatic vessels provide a favorable environment for metastasis of $CD133^+$ melanoma cells.

Published OnlineFirst November 5, 2010; DOI: 10.1158/0008-5472.CAN-10-2591

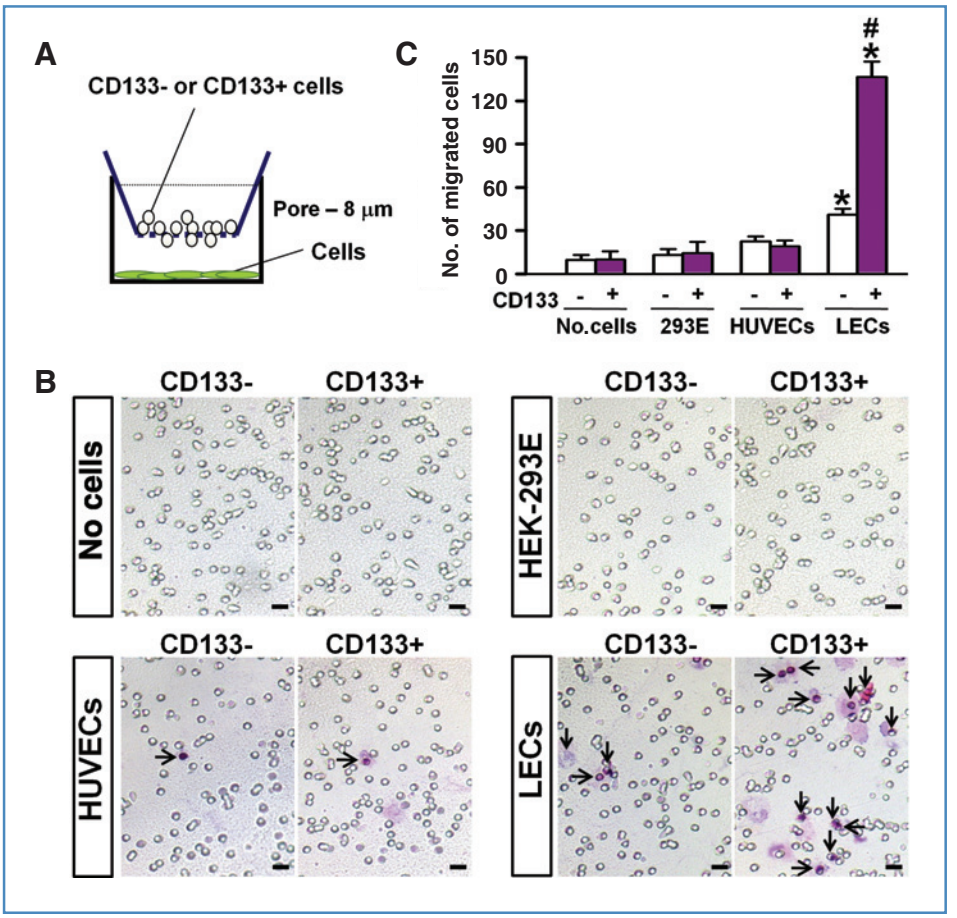

Figure 2. LECs promote migration of CD133$^+$ melanoma cells. A, schematic diagram of the modified Boyden chamber assay to assess migratory capacity of CD133$^+$ and CD133$^-$ cells. Indicated cultured cells, including LECs, are seeded in the bottom of the chamber and freshly isolated CD133$^+$ and CD133$^-$ cells from tumor are loaded onto the upper layer of the membrane with 8 μm pores. B and C, the migratory activity of CD133$^+$ or CD133$^-$ cells assessed in the presence or absence of indicated cells in the lower chamber. After 24 hours of incubation, the transmigrated cells were stained in hematoxylin and eosin solution (B) and number of transmigrated CD133$^+$ or CD133$^-$ cells (arrows, purple) was counted (C). *, $P < 0.05$ versus CD133$^-$ cells/HUVECs or CD133$^+$ cells/HUVECs; #, $P < 0.05$ versus CD133$^-$ cells/LECs. Scale bar, 200 μm.

Lymphatic endothelial cells promote migration of CD133$^+$ melanoma cells

To validate that lymphatic vessels promote the migration of CD133$^+$ tumor cells, we next investigated whether primary cultured LECs facilitate the migratory activity of CD133$^+$ melanoma cells using an *in vitro* Boyden chamber assay (Fig. 2A). Control cells, HUVECs and HEK-293E cells, did not significantly affect the migration of either CD133$^+$ or CD133$^-$ cells (Fig. 2B and C). However, compared with HUVECs, LECs robustly promoted (~7.2-fold) the migratory activity of CD133$^+$ tumor cells rather than CD133$^-$ cells (~1.8-fold; Fig. 2B and C). This result demonstrates that LECs play a substantial role in mediating the migration of CD133$^+$ melanoma cells.

Lymphatic vessels regulate metastasis of CD133$^+$ tumor cells *in vivo*

On the basis of aforementioned findings, we questioned whether the modulation of lymphatic growth could regulate CD133$^+$ tumor cell metastasis *in vivo*. To answer this question, we reduced lymphatic growth through the blockade of VEGF-C/VEGFR-3 signaling by Ad-sVEGFR-3 (30). Conversely, K14-VEGF-C transgenic mice (28), which have dense and enlarged lymphatic vessels in the skin dermis, were used to see the effects of increased lymphatic growth in tumor metastasis. As we expected, Ad-sVEGFR-3 delivery reduced both lymphatic density and blood vessel density in tumor, compared with adenoviral βgal delivery (Ad-βgal); whereas melanoma-bearing K14-VEGF-C transgenic mice showed a profound increase in lymphatic density in tumor, compared with wild-type (WT) littermate mice (Supplementary Fig. S4C–F). Growth of lymphatic vessels rather than blood vessels was remarkably decreased in ALNs after Ad-sVEGFR-3 treatment and, in an adverse manner, K14-VEGF-C transgenic mice showed a significant increase in lymphatic density in ALNs (Fig. 3A and B and Supplementary Fig. S4G). Both Ad-sVEGFR-3 treatment and K14-VEGF-C transgenic phenotype had no impact on either tumor growth or percentage of CD133$^+$ cell population in tumor (Supplementary Fig. S4A and B). Importantly, CD133$^+$/MelanA$^+$ cell metastasis to ALNs was 81% less after administration of Ad-sVEGFR-3 compared with Ad-βgal, but it was increased approximately 2.4-fold in K14-VEGF-C transgenic mice compared with WT mice with melanoma (Fig. 3C–E).

Moreover, compared with Ad-βgal, the number of tumor colonies was 85% less in Ad-sVEGFR-3–treated mice whereas pulmonary metastasis increased approximately 2.1-fold in the lungs of K14-VEGF-C transgenic mice (Fig. 3F). Interestingly, quantitative real-time PCR of RNA isolated from CD133$^+$ cells

Published OnlineFirst November 5, 2010; DOI: 10.1158/0008-5472.CAN-10-2591

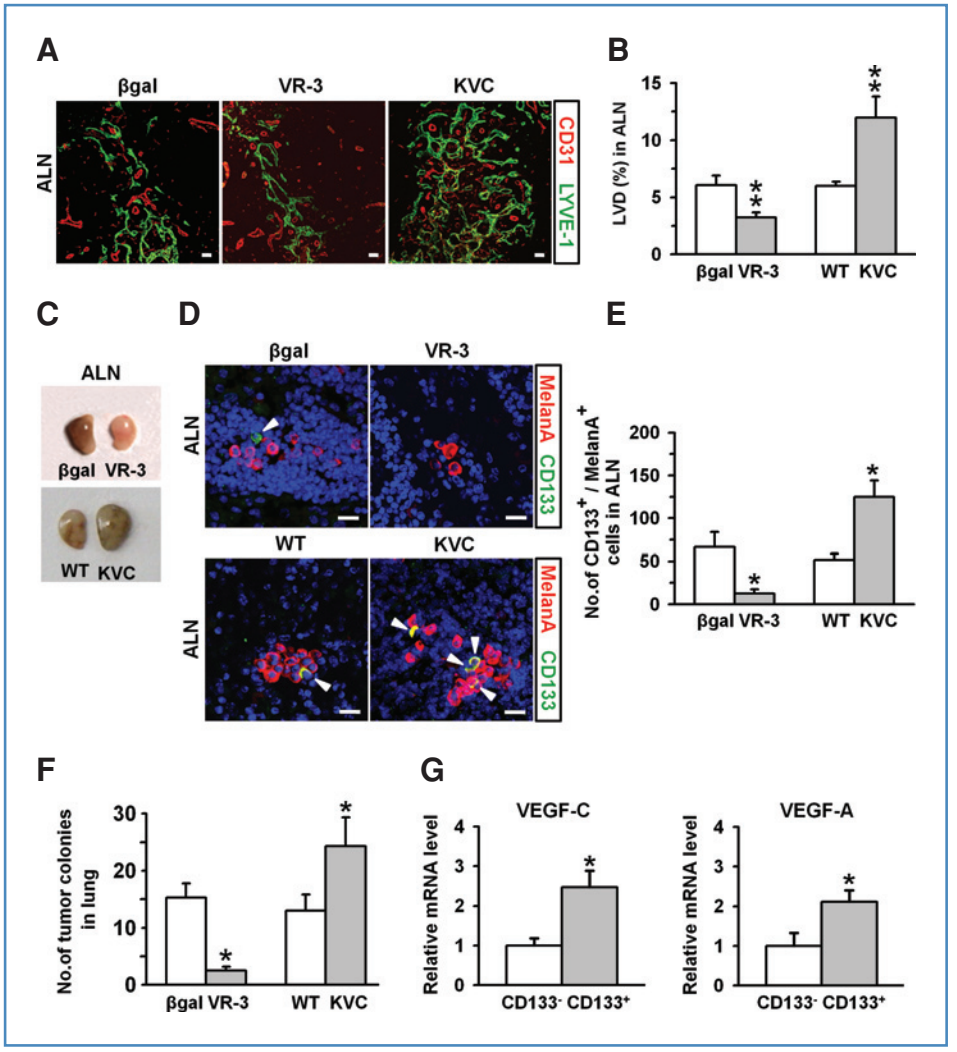

Figure 3. Lymphatic vessels regulate metastasis of CD133$^+$ melanoma cells *in vivo*. Three days after B16/F10 melanoma cells were implanted into C57BL/6J mice, the mice were given intravenous injections of 10^9 pfu of Ad-sVEGFR-3 (VR-3) or Ad-βgal (βgal) every week. B16/F10 melanoma cells were implanted into K14-VEGF-C (KVC) and WT littermate mice. On day 21 after tumor implantation, tumors, ALNs, and lungs were harvested. A and B, images showing differences in the LYVE-1$^+$ lymphatic vessel density (LVD) in ALN (A) and quantification of LVD in ALN (B). Scale bars, 50 μm. **, $P < 0.01$ versus βgal or WT. C, images showing comparisons of ALN sizes. D and E, images showing differences in the metastasis of CD133$^+$/MelanA$^+$ tumor cells in ALN (D) and comparison of the number of CD133$^+$/MelanA$^+$ cells in the mid-sectioned ALN (E). Scale bars, 20 μm. *, $P < 0.05$ versus βgal or WT. F, comparison of the number of tumor colonies in the lung section. *, $P < 0.05$ versus βgal or WT. G, comparisons of VEGF-C and VEGF-A mRNA expressions in the CD133$^+$ and CD133$^-$ cells from tumor. Each group, $n = 6$. *, $P < 0.05$ versus CD133$^-$ cells.

and CD133$^-$ cells of developed tumor revealed that the mRNA expression levels of lymphangiogenic factors, such as VEGF-C and VEGF-A, were higher in CD133$^+$ cells compared with CD133$^-$ cells in tumor (Fig. 3G). In addition, flow cytometric analysis revealed that only ~2.6% and ~3.8% of CD45$^-$/CD133$^+$ tumor cells expressed VEGFR-2 and VEGFR-3, respectively, in tumor (Supplementary Fig. S5). Our results suggest that VEGF-C and VEGF-A released from CD133$^+$ melanoma cells may be actively participating in promoting lymphangiogenesis, therefore facilitating tumor metastasis through lymphatic vessels.

SDF-1/CXCR4 axis is involved in CD133$^+$ tumor cell metastasis toward a lymphatic metastatic niche

Because a strong correlation between tumor metastasis and SDF-1 expression in target organs is reported in some cancers (18), we next investigated whether the SDF-1/CXCR4 axis is involved in the interaction between CD133$^+$ cells and lymphatic vessels, and contributes to forming a lymphatic metastatic niche for guiding CD133$^+$ tumor cell metastasis. For this purpose, we first examined the expression of SDF-1 on lymphatic vessels in metastatic tissues. Immunofluorescence staining showed strong expression of SDF-1 on lymphatic vessels in the metastasized ALNs of tumor-implanted mice, whereas its expression was weak and undetectable in lymphatic vessels of normal ALNs of mice without tumor implantation (Fig. 4A). Strong SDF-1 expression was also observed in lymphatic vessels of either primary tumor or metastasized lungs, but not in other tissues of the melanoma-bearing mice (Supplementary Fig. S6A). In agreement with these findings, SDF-1 and VEGFR-3 mRNA expression levels were, respectively, approximately 6.6- and 3.8-fold higher in the ALNs and were approximately 3.8- and 2.2-fold higher in lung tissues of melanoma-bearing mice compared with normal mice (Supplementary Fig. S6B). However, their expression levels were not significantly changed in other organs, such as liver, spleen, and testis, in which metastasis was infrequently observed after tumor implantation (Supplementary Fig. S6B and data not

Published OnlineFirst November 5, 2010; DOI: 10.1158/0008-5472.CAN-10-2591

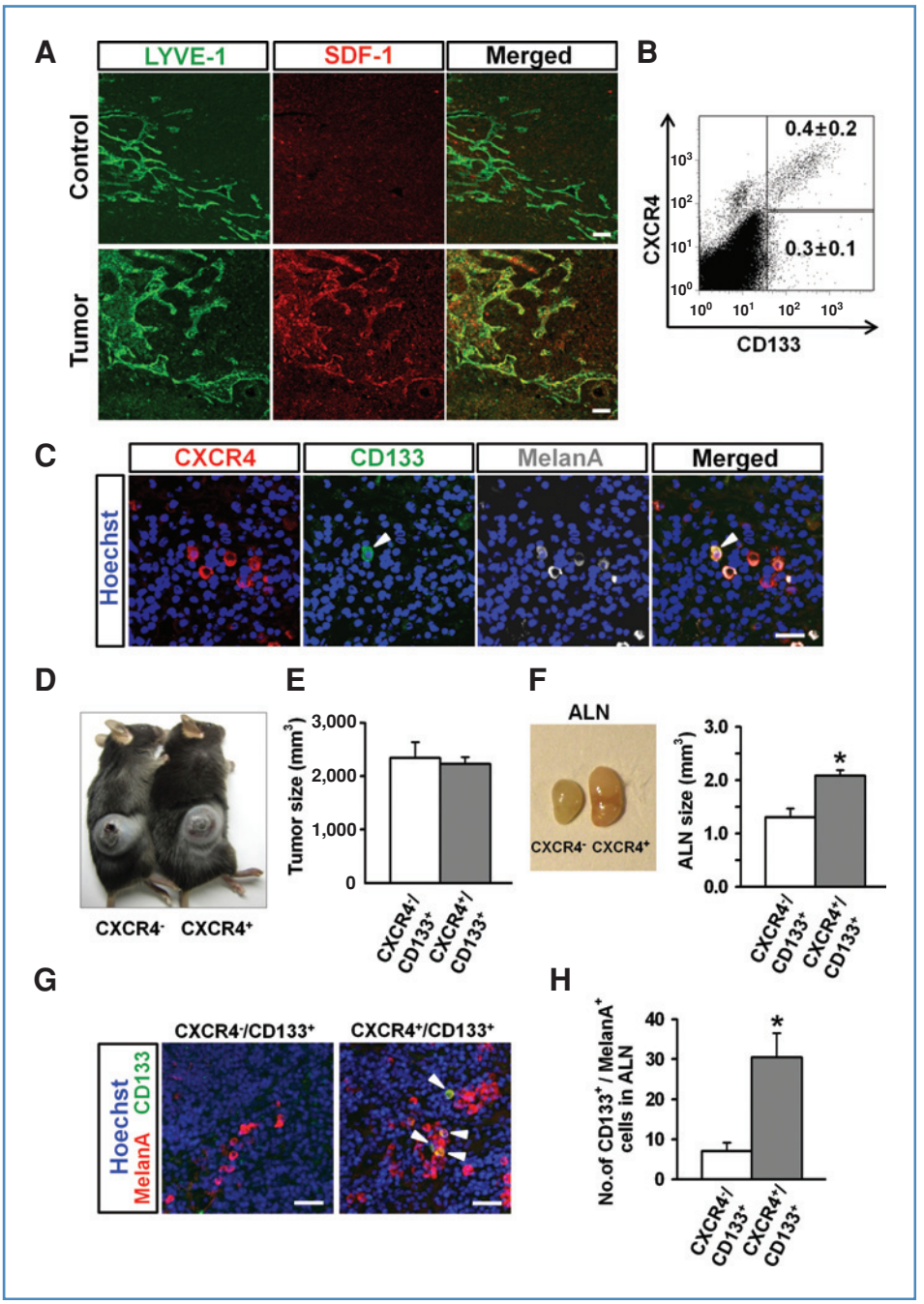

Figure 4. SDF-1/CXCR4 axis is involved in CD133$^+$ tumor cell metastasis toward a lymphatic metastasis niche. A–C, 3 weeks after B16/F10 melanoma cells were implanted into C57BL/6J mice, the tumors, and ALNs were harvested. A, images showing differences in SDF-1 expression on LYVE-1$^+$ lymphatic vessels in control and metastasized ALNs. Scale bars, 50 μm. B, FACS analysis of CXCR4 expression on CD133$^+$ cells in tumor. C, images showing CD133$^+$/MelanA$^+$ cells coexpressing CXCR4 in ALN (arrowheads). Each group, $n = 6$. Scale bar, 20 μm. D–H, 2 weeks after 1×10^3 of sorted CXCR4$^+$/CD133$^+$ and CXCR4$^-$ /CD133$^+$ cells were implanted into C57BL/6J mice, tumor volumes were measured, and the tumors and ALNs were sampled. D and E, photograph showing the gross features of tumor formation (D) and quantification of tumor size (E). F, photograph showing gross features of metastasized ALN (left) and quantification of LN size (right). *, $P < 0.05$ versus CXCR4$^-$/CD133$^+$ cells. G and H, images showing differences CD133$^+$/MelanA$^+$ cell (white arrowheads) metastasis to ALN (G) and quantification of the number of CD133$^+$/MelanA$^+$ cells in the mid-sectioned ALN (H). Scale bars, 20 μm. Each group, $n = 6$. *, $P < 0.05$ versus CXCR4$^-$/CD133$^+$ cells.

shown). These findings led us to assess the expression of CXCR4, a specific receptor for SDF-1, particularly in CD133$^+$ melanoma cells. Flow cytometric analysis showed that a distinct population of CD133$^+$ cells (57.9%) expressed CXCR4 in tumor (Fig. 4B). Furthermore, immunofluorescence costaining confirmed that a certain set of CD133$^+$/MelanA$^+$ cells in the ALNs express CXCR4 (Fig. 4C). On the basis of these findings, we hypothesized that the CXCR4-expressing CD133$^+$ tumor cells may have high metastatic activity. To test this hypothesis, we isolated CXCR4$^+$/CD133$^+$ and CXCR4$^-$/CD133$^+$ cells from the tumor using FACS and injected 1×10^3 cells of each population subcutaneously into mice. We then measured tumor growth and metastasis 2 weeks after implantation. Notably, melanoma formed by CXCR4$^+$/CD133$^+$ cell implantation exerted approximately 1.6-fold larger ALN size and approximately 4.4-fold higher CD133$^+$ cell metastasis to the ALNs compared with the melanoma formed by CXCR4$^-$/CD133$^+$ cell implantation (Fig. 4F–H), even though both groups showed similar extents of tumor growth (Fig. 4D and E). These results indicate that SDF-1 mediates

Published OnlineFirst November 5, 2010; DOI: 10.1158/0008-5472.CAN-10-2591

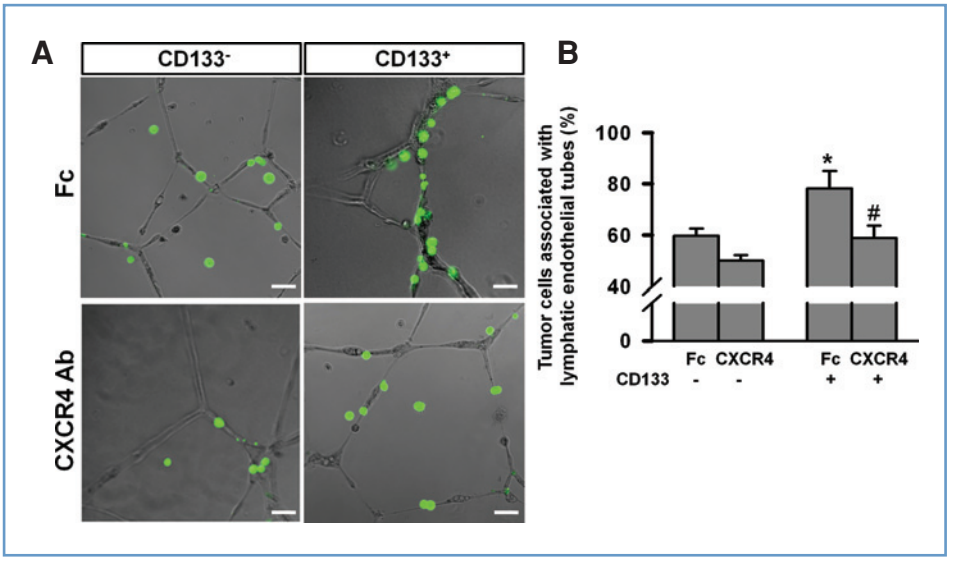

Figure 5. Blockade of CXCR4 signaling reduces physical association of CD133$^+$ cells to LECs. Unlabeled LECs were cocultured for 24 hours with CFDA SE-labeled CD133$^+$ or CD133$^-$ cells, which were freshly isolated from tumor. CXCR4 blocking antibody (500 ng/mL) or Fc was administered after seeding of mixed cells on the Matrigel-coated plates. A, overlay of phase-contrast and fluorescence images showing differences in association of CD133$^+$ (green) or CD133$^-$ cells (green) to LECs. Scale bars, 50 μm. B, percentage of CD133$^+$ or CD133$^-$ cells which are associated with unlabeled LECs per total CD133$^+$ or CD133$^-$ cells in each well. *, $P < 0.05$ versus Fc-treated CD133$^-$ cells; #, $P < 0.05$ versus Fc-treated CD133$^+$ cells.

CD133$^+$ cell metastasis toward a lymphatic metastatic niche in target organs.

Blockade of CXCR4 signaling reduces physical association of CD133$^+$ cells to LECs

To demonstrate whether CXCR4 signaling is a responsible mediator for physical association between CD133$^+$ tumor cells and LECs, freshly isolated CD133$^+$ and CD133$^-$ cells from tumor were labeled with a green fluorescent dye CFDA-SE and cocultured with LECs in Matrigel for 24 hours. We observed that, compared with CD133$^-$ cells, CD133$^+$ tumor cells associated more closely with LECs (Fig. 5A and B). Importantly, blockade of CXCR4 with anti-CXCR4 blocking antibody significantly impaired the association between CD133$^+$ tumor cells and LECs by 25%, whereas the association between CD133$^-$ tumor cells and LECs was only slightly affected after CXCR4 blockade (Fig. 5A and B).

Blockade of CXCR4 signaling suppresses tumor metastasis to the ALNs and lungs

To confirm that CXCR4 signaling is responsible for melanoma metastasis, especially of the chemoresistant CD133$^+$ cells, we administered a CXCR4 inhibitor AMD3100 and a cytotoxic chemotherapeutic agent dacarbazine 1 week after melanoma implantation. Blocking CXCR4 signaling with AMD3100 did not significantly affect either tumor growth or percentage of CD133$^+$ cell population in tumor (Fig. 6A–C), but it significantly reduced CD133$^+$ tumor cell metastasis to ALNs and pulmonary metastasis, compared with the vehicle (Fig. 6D–G). The number of tumor cells surrounding lymphatic vessels in the lungs was also reduced by AMD3100 treatment (Fig. 6E). In comparison, dacarbazine alone or combined treatment of AMD3100 plus dacarbazine increased the percentage of CD133$^+$ cell population in tumor by approximately 5.8- and 5.7-fold, respectively, compared with the vehicle (Fig. 6C). In terms of metastasis, as we expected, dacarbazine treatment alone could not block metastasis to the ALNs and lungs although it reduced tumor growth by 55% (Fig. 6A and B). However, importantly, combined treatment of AMD3100 plus dacarbazine showed a significant reduction in tumor metastasis either to ALNs by 62% or to lungs by 49% and also induced a decrease in the number of tumor cells surrounding lymphatic vessels in the lungs (Fig. 6D–G). Together, our results confirm that CXCR4 signaling is a crucial pathway in regulating metastatic activity of chemoresistant CD133$^+$ tumor cells toward a lymphatic niche in target metastatic organs (Supplementary Fig. S7). Therefore, the blockade of CXCR4 signaling plus dacarbazine administration suppresses the highly metastatic phenotype of melanoma, which remains as a significant problem with dacarbazine treatment alone.

Discussion

The underlying mechanisms of highly metastatic and chemoresistant characteristics of malignant melanomas are still poorly understood for the development of an effective treatment. Our study identifies a distinct population expressing CD133 (Prominin-1) that is highly enriched after repeated exposure of a chemotherapeutic drug, which may lead to the selection of certain tumor subsets. Importantly, our data demonstrate that lymphatic microenvironments actively regulate metastasis of CD133$^+$ cells with high metastatic potential by a specific signaling pathway *in vivo* (Supplementary Fig. S7).

Published OnlineFirst November 5, 2010; DOI: 10.1158/0008-5472.CAN-10-2591

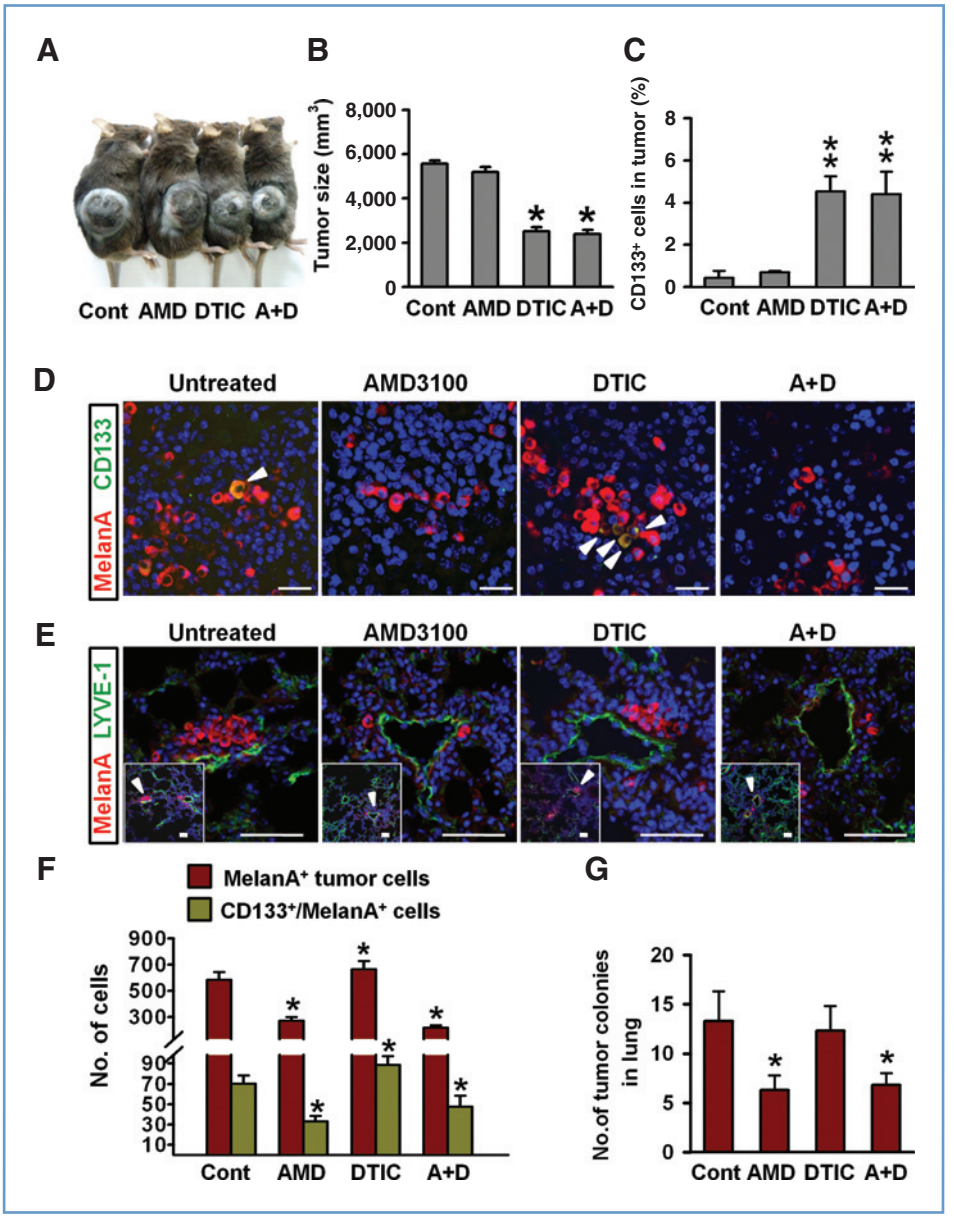

Figure 6. Blockade of CXCR4 signaling suppresses tumor metastasis to the ALNs and lung. Seven days after B16/F10 melanoma cells were implanted into C57BL/6J mice, AMD3100 (every 2 days 1.25 mg/kg subcutaneously) alone, dacarbazine (DTIC, 50 mg/kg intraperitoneally) alone, combined treatment of AMD3100 plus dacarbazine (A+D), or vehicle treatment (Cont) was given. 14 days after treatment, tumor volumes were measured, and the tumors, ALNs, and lungs were sampled. A and B, photographs showing gross features of tumor growths (A) and quantification of tumor sizes (B). *, $P < 0.05$ versus Cont. C, FACS analysis of percentage of $CD133^+$ cells in total tumor cells. **, $P < 0.01$ versus Cont. D, images showing differences in $CD133^+/MelanA^+$ tumor cell metastasis (white arrowheads) to ALN after drug treatment. Scale bars, 20 μm. E, images showing $MelanA^+$ tumor cells adjacent to LYVE-1$^+$ lymphatic vessels in the lung sections. Indicated regions by white arrowhead in each inset are magnified. Scale bars, 50 μm. F, the number of $MelanA^+$ tumor cells and $CD133^+/MelanA^+$ cells in the mid-sectioned ALN. G, the number of tumor colonies (defined as >20 $MelanA^+$ cells) in the lung sections. Each group, $n = 5$. *, $P < 0.05$ versus Cont.

$CD133^+$ tumor cells represent the cellular population that confers radio and chemoresistance and could be the source of tumor recurrence after therapeutic treatments (7, 31). Our study confirmed that, *in vivo*, the $CD133^+$ subpopulation is highly enriched in a melanoma model after administration of dacarbazine, which is generally considered to be the most active agent for treating malignant melanoma. Our goal was not to determine whether chemotherapeutic resistance correlates with the ability of melanoma subsets to form tumors, but rather to elucidate precise mechanisms determining the directional metastasis of $CD133^+$ tumor cells to specific target organs. It is reported that angiogenesis and metastasis are enhanced after dacarbazine administration to melanoma (6). Our data further identified that lymphatic growth, both in tumor and in regional LNs, increased after dacarbazine treatment *in vivo*. These observations led us to examine the potential role of lymphatic vessels as microenvironments to guide metastatic $CD133^+$ tumor cells with chemoresistance to target organs. Previous reports have shown that tumor-associated cells, such as hematopoietic progenitor cells and inflammatory cells, create a conducive microenvironment for tumor metastasis (32, 33). In our study, we discovered that the distribution of $CD133^+/MelanA^+$ tumor cells is primarily toward lymphatic vessels in metastasized LNs, suggesting that tumor-associated lymphatic vasculature in LNs can establish proper environments to promote the metastasis of $CD133^+$ tumor cells. For the preferred target organ of melanoma metastasis, the lungs, $CD133^+/MelanA^+$ cells colocalized with other $MelanA^+$ tumor

Published OnlineFirst November 5, 2010; DOI: 10.1158/0008-5472.CAN-10-2591

cells by forming colonies. Also, as we emphasize in this study, a certain set of $CD133^+$ tumor cells was observed to closely surround lymphatic vessels in the metastasized lung. This phenomenon suggests the role of lymphatic vasculature in facilitating lymphatic spread of $CD133^+$ melanoma cells in the lungs. Notably, we found that reduction or promotion of lymphatic vessel growth, respectively, attenuated or enhanced $CD133^+$ cell metastasis to the regional LN and lung metastasis. Moreover, the number of $MelanA^+$ tumor cells that closely reside adjacent to lymphatic vessels decreased in the lung after Ad-sVEGFR-3 treatment (data not shown). The modulation of lymphatic growth, however, did not affect the percentage of $CD133^+$ population in tumor, implying that lymphatic vessels do not regulate the maintenance of $CD133^+$ tumor cells but rather are principally responsible for $CD133^+$ melanoma cell metastasis. Furthermore, $CD133^+$ cells were observed to express higher mRNA levels of lymphangiogenic factors, VEGF-C and VEGF-A, compared with $CD133^-$ cells in tumor. These results explain that $CD133^+$ melanoma cells can promote lymphangiogenesis in metastatic tissues as well as in primary tumor by strongly expressing lymphangiogenic factors, therefore facilitating tumor metastasis through the lymphatic system.

Tumor metastasis is a dynamic process involving multiple molecular and cellular mechanisms (34). Recent studies have shown that local molecular and cellular components of metastatic tissues can create a favorable niche and adjust the metastatic activity of disseminating tumor cells to favorable organs (15, 16). Chemokine-mediated mechanisms have also been proposed to promote metastasis to specific target destinations by acting directly on tumor cell migration. For example, the chemokine CCL21 released from LECs stimulates the migration of melanoma cells into the lymphatic system (19).

The SDF-1/CXCR4 axis mainly implicates homing of stem cells into the bone marrow (35). Previous studies have indicated a strong correlation between the SDF-1/CXCR4 axis and tumor metastasis and have demonstrated that the gradient of SDF-1 expression can regulate tumor cell invasion to specific anatomic sites (17, 18). Indeed, our results revealed that expression levels of SDF-1 mRNA are highly increased in preferred metastatic sites such as LNs and lungs. Furthermore, as a novel source for SDF-1, lymphatic vessels either in tumor or in metastatic sites were observed to strongly express SDF-1 compared with nontumor-bearing mice. In tumor, a high frequency of $CD133^+$ cells (~60%) was seen to express CXCR4, indicating that SDF-1 in metastatic tissues may create receptive microenvironments for the recruitment of CXCR4-expressing $CD133^+$ cells from the primary tumoral region. At the same time, this result suggests that a distinct population of $CD133^+$ cells has high metastatic activity by expressing CXCR4. Indeed, further studies based on this finding demonstrated that CXCR4-expressing $CD133^+$ cells exhibit enhanced metastasis compared with $CXCR4^-/CD133^+$ cells *in vivo*. Our findings show that CXCR4 importantly mediates chemotactic and metastatic responses of $CD133^+$ cells *in vivo*. As discussed above, treatment of melanoma gives rise to poor response rates resulting from a highly resistant and metastatic phenotype. Our results correspondingly show that dacarbazine does not attenuate LN and pulmonary metastases, despite its ability to reduce tumor growth. Considering our results, the blockade of CXCR4 signaling coupled with dacarbazine treatment *in vivo* is promising as a new therapeutic strategy for treating melanoma. Specifically, blocking the CXCR4 signaling in addition to dacarbazine administration significantly impaired $CD133^+$ cell migration, resulting in decreased LN and pulmonary metastases.

In conclusion, our study demonstrates the role of a lymphatic microenvironment at preferred metastatic sites in guiding metastasis of a distinct tumor subset expressing CD133 that is enriched after dacarbazine treatment. Here, the SDF-1/CXCR4 axis is essential for the functionality of the lymphatic metastatic niche that attracts CXCR4-expressing tumor cells. We unraveled the role of lymphatic vessels as a novel source of SDF-1, which promotes the metastasis of CXCR4-expressing $CD133^+$ cells (Supplementary Fig. S7). Importantly, the blockade of CXCR4 signaling coupled with dacarbazine treatment impaired LN and pulmonary metastases as well as tumor growth. Thus, our findings suggest that targeting the SDF-1/CXCR4 axis, a key regulator of the lymphatic niche, will lead to a novel combinational therapy with dacarbazine by blocking the metastasis of chemoresistant $CD133^+$ cells.

Disclosure of Potential Conflicts of Interest

No potential conflicts of interest were disclosed.

Acknowledgment

We thank Jin Sun Hong and Eun Soon Lee for their technical assistance.

Grant Support

This study was supported by a grant (A092255, GYK) of the Korea Healthcare technology R&D Project, Ministry for Health & Welfare Affairs, Korea.

The costs of publication of this article were defrayed in part by the payment of page charges. This article must therefore be hereby marked *advertisement* in accordance with 18 U.S.C. Section 1734 solely to indicate this fact.

Received 07/16/2010; revised 10/12/2010; accepted 10/22/2010; published OnlineFirst 11/05/2010.

References

1. Chin L, Garraway LA, Fisher DE. Malignant melanoma: genetics and therapeutics in the genomic era. Genes Dev 2006;20:2149–82.
2. Soengas MS, Lowe SW. Apoptosis and melanoma chemoresistance. Oncogene 2003;22:3138–51.
3. Cassel WA, Olkowski ZL, Murray DR. Immunotherapy in malignant melanoma. J Clin Oncol 1999;17:1963.
4. McMasters KM, Swetter SM. Current management of melanoma: benefits of surgical staging and adjuvant therapy. J Surg Oncol 2003;82:209–16.

Published OnlineFirst November 5, 2010; DOI: 10.1158/0008-5472.CAN-10-2591

5. Middleton MR, Grob JJ, Aaronson N, Fierlbeck G, Tilgen W, Seiter S, et al. Randomized phase III study of temozolomide versus dacarbazine in the treatment of patients with advanced metastatic malignant melanoma. J Clin Oncol 2000;18:158–66.
6. Lev DC, Onn A, Melinkova VO, Miller C, Stone V, Ruiz M, et al. Exposure of melanoma cells to dacarbazine results in enhanced tumor growth and metastasis *in vivo*. J Clin Oncol 2004;22:2092–100.
7. Bao S, Wu Q, McLendon RE, Hao Y, Shi Q, Hjelmeland AB, et al. Glioma stem cells promote radioresistance by preferential activation of the DNA damage response. Nature 2006;444:756–60.
8. Todaro M, Alea MP, Di Stefano AB, Cammareri P, Vermeulen L, Iovino F, et al. Colon cancer stem cells dictate tumor growth and resist cell death by production of interleukin-4. Cell Stem Cell 2007;1:389–402.
9. Frank NY, Margaryan A, Huang Y, Schatton T, Waaga-Gasser AM, Gasser M, et al. ABCB5-mediated doxorubicin transport and chemoresistance in human malignant melanoma. Cancer Res 2005;65:4320–33.
10. Schatton T, Murphy GF, Frank NY, Yamaura K, Waaga-Gasser AM, Gasser M, et al. Identification of cells initiating human melanomas. Nature 2008;451:345–9.
11. Held MA, Curley DP, Dankort D, McMahon M, Muthusamy V, Bosenberg MW. Characterization of melanoma cells capable of propagating tumors from a single cell. Cancer Res 2010;70:388–97.
12. Quintana E, Shackleton M, Sabel MS, Fullen DR, Johnson TM, Morrison SJ. Efficient tumour formation by single human melanoma cells. Nature 2008;456:593–8.
13. Boiko AD, Razorenova OV, van de Rijn M, Swetter SM, Johnson DL, Ly DP, et al. Human melanoma-initiating cells express neural crest nerve growth factor receptor CD271. Nature 2010;466:133–7.
14. Nguyen DX, Bos PD, Massague J. Metastasis: from dissemination to organ-specific colonization. Nat Rev Cancer 2009;9:274–84.
15. Joyce JA, Pollard JW. Microenvironmental regulation of metastasis. Nat Rev Cancer 2009;9:239–52.
16. Psaila B, Lyden D. The metastatic niche: adapting the foreign soil. Nat Rev Cancer 2009;9:285–93.
17. Li YM, Pan Y, Wei Y, Cheng X, Zhou BP, Tan M, et al. Upregulation of CXCR4 is essential for HER2-mediated tumor metastasis. Cancer Cell 2004;6:459–69.
18. Muller A, Homey B, Soto H, Ge N, Catron D, Buchanan ME, et al. Involvement of chemokine receptors in breast cancer metastasis. Nature 2001;410:50–6.
19. Shields JD, Emmett MS, Dunn DB, Joory KD, Sage LM, Rigby H, et al. Chemokine-mediated migration of melanoma cells towards lymphatics–a mechanism contributing to metastasis. Oncogene 2007;26:2997–3005.
20. Stacker SA, Baldwin ME, Achen MG. The role of tumor lymphangiogenesis in metastatic spread. FASEB J 2002;16:922–34.
21. Mandriota SJ, Jussila L, Jeltsch M, Compagni A, Baetens D, Prevo R, et al. Vascular endothelial growth factor-C-mediated lymphangiogenesis promotes tumour metastasis. EMBO J 2001;20:672–82.
22. Alitalo K, Tammela T, Petrova TV. Lymphangiogenesis in development and human disease. Nature 2005;438:946–53.
23. Meier F, Will S, Ellwanger U, Schlagenhauff B, Schittek B, Rassner G, et al. Metastatic pathways and time courses in the orderly progression of cutaneous melanoma. Br J Dermatol 2002;147:62–70.
24. Tammela T, Alitalo K. Lymphangiogenesis: molecular mechanisms and future promise. Cell 2010;140:460–76.
25. Lin J, Lalani AS, Harding TC, Gonzalez M, Wu WW, Luan B, et al. Inhibition of lymphogenous metastasis using adeno-associated virus-mediated gene transfer of a soluble VEGFR-3 decoy receptor. Cancer Res 2005;65:6901–9.
26. Krishnan J, Kirkin V, Steffen A, Hegen M, Weih D, Tomarev S, et al. Differential *in vivo* and *in vitro* expression of vascular endothelial growth factor (VEGF)-C and VEGF-D in tumors and its relationship to lymphatic metastasis in immunocompetent rats. Cancer Res 2003;63:713–22.
27. Das S, Ladell DS, Podgrabinska S, Ponomarev V, Nagi C, Fallon JT, et al. Vascular endothelial growth factor-C induces lymphangitic carcinomatosis, an extremely aggressive form of lung metastases. Cancer Res 2010;70:1814–24.
28. Jeltsch M, Kaipainen A, Joukov V, Meng X, Lakso M, Rauvala H, et al. Hyperplasia of lymphatic vessels in VEGF-C transgenic mice. Science 1997;276:1423–5.
29. Levina V, Marrangoni AM, DeMarco R, Gorelik E, Lokshin AE. Drug-selected human lung cancer stem cells: cytokine network, tumorigenic and metastatic properties. PLoS One 2008;3:e3077.
30. Makinen T, Jussila L, Veikkola T, Karpanen T, Kettunen MI, Pulkkanen KJ, et al. Inhibition of lymphangiogenesis with resulting lymphedema in transgenic mice expressing soluble VEGF receptor-3. Nat Med 2001;7:199–205.
31. Dean M, Fojo T, Bates S. Tumour stem cells and drug resistance. Nat Rev Cancer 2005;5:275–84.
32. Kaplan RN, Riba RD, Zacharoulis S, Bramley AH, Vincent L, Costa C, et al. VEGFR1-positive haematopoietic bone marrow progenitors initiate the pre-metastatic niche. Nature 2005;438:820–7.
33. Coussens LM, Werb Z. Inflammation and cancer. Nature 2002;420:860–7.
34. Chambers AF, Groom AC, MacDonald IC. Dissemination and growth of cancer cells in metastatic sites. Nat Rev Cancer 2002;2:563–72.
35. Loetscher P, Moser B, Baggiolini M. Chemokines and their receptors in lymphocyte traffic and HIV infection. Adv Immunol 2000;74:127–80.

Published OnlineFirst November 5, 2010; DOI: 10.1158/0008-5472.CAN-10-2591

Cancer Research
The Journal of Cancer Research (1916–1930) | The American Journal of Cancer (1931–1940)

AACR American Association for Cancer Research

CXCR4 Signaling Regulates Metastasis of Chemoresistant Melanoma Cells by a Lymphatic Metastatic Niche

Minah Kim, Young Jun Koh, Kyung Eun Kim, et al.

Cancer Res 2010;70:10411-10421. Published OnlineFirst November 5, 2010.